

MicroSPECT/CT Imaging and Pharmacokinetics of ^{188}Re -(DXR)-liposome in Human Colorectal Adenocarcinoma-bearing Mice

MIN-HUA CHEN^{1,3}, CHIH-HSIEN CHANG², YA-JEN CHANG², LIANG-CHENG CHEN²,
CHIA-YU YU², YU-HSIEN WU², WAN-CHI LEE², CHUNG-HSIN YEH²,
FENG-HUEI LIN³, TE-WEI LEE², CHUNG-SHI YANG¹ and GANN TING¹

¹Center of Nanomedicine Research, National Health Research Institutes, Miaoli, Taiwan;

²Institute of Nuclear Energy Research, Taoyuan, Taiwan;

³Institute of Biomedical Engineering, National Taiwan University, Taipei, Taiwan, R.O.C.

Abstract. Nanoliposome can be designed as a drug delivery carrier to improve the pharmacological and therapeutic properties of drug administration. ^{188}Re -labeled nanoliposomes are useful for diagnostic imaging as well as for targeted radionuclide therapy. In this study, the *in vivo* nuclear imaging, pharmacokinetics and biodistribution of administered nanoliposomes were investigated as drug and radionuclide carriers for targeting solid tumor via intravenous (*i.v.*) administration. The radiotherapeutics (^{188}Re -liposome) and radiochemotherapeutics (^{188}Re -DXR-liposome) were *i.v.* administered to nude mice bearing human HT-29 colorectal adenocarcinoma xenografts. ^{188}Re -liposome and ^{188}Re -DXR-liposomes show similar biodistribution profile; both have higher tumor uptake, higher blood retention time, and lower excretion rate than ^{188}Re -N,N-bis(2-mercaptoethyl)-N',N'-diethylenediamine (BMEDA). In contrast to tumor uptake, the area under the curve (AUC) value of tumor for ^{188}Re -liposome and ^{188}Re -DXR-liposome was 16.5- and 11.5-fold higher than that of free ^{188}Re -BMEDA, respectively. Additionally, ^{188}Re -liposome and ^{188}Re -DXR-liposome had a higher tumor-to-muscle ratio at 24 h (14.4 ± 0.7 and 17.14 ± 4.1 , respectively) than ^{188}Re -BMEDA (1.6 ± 0.1). The tumor targeting and distribution of ^{188}Re -(DXR)-liposome (representing ^{188}Re -DXR-liposome and ^{188}Re -liposome) can also be acquired by signal photon-emission computed tomography/computed tomography images

as well as whole body autoradiograph. These results suggest that ^{188}Re -(DXR)-liposomes are potentially promising agents for passive targeting treatment of malignant disease.

Colorectal cancer is highly prevalent and a common cause of cancer in Taiwan, fourth most common malignancy in the United States, and is the second leading cause of cancer-related death (1, 2). It is currently very attractive to develop anticancer drug delivery system for cancer therapy. Nanoparticles can be designed as a drug delivery system to improve the pharmacological and therapeutic properties of drug administration through the enhanced permeability and retention effect (EPR) in tumor sites (3). Several types of carriers have been developed in the last few decades, these include nanoliposomes, carbon nanotubes, micelles, dendrimers, iron oxides and quantum dots (4, 5).

Liposomes are well known to the medical community, particularly as drug carriers for cancer treatment. Nanoliposomes alter the pharmacokinetics and biodistribution of free drugs and function as a reservoir for sustained drug release. Moreover, the leaky vasculature and lack of a well-defined lymphatic system allow intravenously (*i.v.*) administered nanoliposomes to achieve spontaneous accumulation via the EPR effect in tumor sites. The advantages of nanoliposome enable it to cause fewer side-effects than do free drugs alone. To minimize the rate of mononuclear phagocyte system or reticuloendothelial system (RES) uptake for developing a long blood circulation, the most commonly used strategy is to conjugate polyethylene glycol (PEG) polymer, which is a relatively inert hydrophilic polymer that provides good steric hindrance for preventing protein binding onto the surface of the liposome (6-8).

One application of nanoliposome as a carrier system is the encapsulation of therapeutic radionuclides for internal targeted radiotherapy. Chang *et al.* have reported the long retention of ^{188}Re -liposome compared with that of

Correspondence to: Dr. Gann Ting, Center of Nanomedicine Research and National Institute of Cancer Research, National Health Research Institutes, 4F, 123-2, Section 1, Wan-Mei Street, Wen-Shan Districts, Taipei 116, Taiwan. R.O.C. Tel: +886 222308383, Fax: +886 222302573, e-mail: gann.ting@msa.hinet.net

Key Words: Colorectal adenocarcinoma, microSPECT/CT imaging, nanoliposome, pharmacokinetics, ^{188}Re .

unencapsulated ^{188}Re in tumor following *i.v.* injection in C26 tumor-bearing mice (9). Bao *et al.* also reported that $^{99\text{m}}\text{Tc}$ - *N,N*-bis(2-mercaptoethyl)-*N',N'*-diethylenediamine (BMEDA) pegylated liposomal doxorubicin and ^{186}Re -BMEDA pegylated liposome have longer half-life in blood than that of unencapsulated $^{99\text{m}}\text{Tc}$ -BMEDA and ^{186}Re -BMEDA after *i.v.* injection in normal mice (10, 11). These preclinical studies clearly indicate that radionuclides encapsulated in liposome are capable of improving the profile of biodistribution and pharmacokinetics for passive target cancer therapy. Moreover, liposome encapsulating γ -emission therapeutic radionuclides ^{111}In , ^{123}I , ^{188}Re and ^{186}Re are able to offer tools as signal photon-emission computed tomography (SPECT) imaging (5). Ogiwara-Umeda *et al.* reported a higher accumulation of small-sized (80 nm) liposome-encapsulated ^{67}Ga -NTA and ^{111}In -NTA in tumor compared with that of free ^{67}Ga , ^{111}In and $^{99\text{m}}\text{Tc}$ (12). Additionally, ^{188}Re is a radionuclide for imaging and therapeutic dual applications due to its short physical half-life of 16.9 h with 155 keV gamma emission for imaging and its 2.12 MeV β emission, with maximum tissue penetration range of 11 mm for tumor therapeutics (9, 13, 14).

Currently, the combination of chemotherapeutic drugs with radiation has been shown to improve survival and locoregional control of various types of cancer compared with radiotherapy alone (15, 16). Several studies have shown significant increase in therapeutic efficacy and reduced toxicity in delivery of chemotherapeutics such as doxorubicin, paclitaxel, epirubicin, vinorelbine and topotecan (17). It is valuable to monitor the pharmacokinetics and biodistribution of nanoliposomes followed by imaging to understand and predict their efficacy and side-effects.

With this in mind, we employed ^{188}Re -liposome (9, 14, 18) and ^{188}Re -DXR-liposome (18, 19) as carriers to estimate the pharmacokinetics and therapeutic efficacy of radionuclide drug in murine C26 colon solid tumor or/and ascites model. However, the ^{188}Re -radiolabeled Lipo-Dox (^{188}Re -DXR-liposome), pharmacokinetics and imaging study of radiochemotherapeutics in human colorectal HT-29 solid tumor model has not been reported yet. Moreover, dual functional and dual modality ^{188}Re -DXR-liposome is a novel nanocarrier for non-invasive simultaneous imaging and therapy (20, 21). In this study, the imaging, pharmacokinetics and biodistribution of administered nanotargeted ^{188}Re -(DXR)-liposomes (representing ^{188}Re -DXR-liposome and ^{188}Re -liposome) were investigated as drug carriers for treating HT-29 solid tumor *via i.v.* administration. This dual functional design of ^{188}Re -(DXR)-liposome can also be used to predict the pharmacological distribution *via* SPECT/CT imaging as well as whole-body autoradiography (WBAR).

Materials and Methods

Materials. Distearoylphosphatidylcholine (DSPC), cholesterol and polyethylene glycol (average M.W. 2000)-derived distearoylphosphatidylethanolamine (PEG-DSPE) were purchased from Avanti Polar Lipids (Alabaster, AL, USA). Cell culture materials were obtained from GIBCO BRL (Grand Island, NY, USA). PD-10 column and Sepharose 4 Fast Flow were purchased from GE Healthcare (Uppsala, Sweden). *N,N*-Bis(2-mercaptoethyl)-*N',N'*-diethylenediamine (BMEDA) were purchased from ABX (Radeberg, Germany). All other chemicals were purchased from Merck (Darmstadt, Germany).

Cell line and animal model. The HT-29 human colorectal adenocarcinoma cell line was purchased from the Bioresource Collection and Research Center, Hsinchu, Taiwan. It was grown in RPMI-1640 medium supplemented with 10% (v/v) fetal bovine serum and 2 mM L-glutamine at 37°C in 5% CO₂. Cells were detached with 0.05% trypsin/0.53 mM EDTA in Hanks' balanced salt solution. Female nude mice (4 to 6 weeks old) were obtained from BioLASCO Taiwan Co. Ltd. (Taipei, Taiwan), with water and food being provided *ad libitum* in the animal house of the Institute of Nuclear Energy Research (Taoyuan, Taiwan). Nude mice were subcutaneously inoculated with 2×10^6 HT-29 cells in the right hind flank. Tumors were measured, individual tumor volumes were calculated by the formula: $V = (\text{length} \times \text{width}^2)/2$.

Nanoliposome preparation. Liposomes were prepared by a lipid film hydration-extrusion method using repeated freeze-thawing to hydrate the lipid films (22). Liposomes were composed of DSPC, cholesterol and methoxy polyethylene glycol (mPEG)-1,2-distearoyl-3-sn-glycerophosphoethanol-amine at a molar ratio of 3:2:0.3. Following hydration in ammonium sulfate solution at 60°C, liposomes were repeatedly extruded through polycarbonate membrane filters (0.2-, 0.1- and 0.05- μm pore sizes) (Costar, Cambridge, MA, USA). The extraliposomal salts were removed by a Sephadex G-50 column (22). Phospholipid concentration was measured by phosphate assay (23). The liposomes were finally analyzed at 14.14 $\mu\text{mol/ml}$ phospholipids having an average particle size of 80.5 ± 14.1 nm.

^{188}Re -(DXR)-liposome preparation. ^{188}Re was obtained as an isotonic solution in the form of sodium perrhenate from an aluminum oxide column by elution with normal saline (24). ^{188}Re -BMEDA was prepared following the method proposed by Bao *et al.* (11). Five mg of BMEDA were dissolved in 0.5 ml of 0.17 mol/l sodium gluconate (in acetate solution) and 120 μl of stannous chloride (10 mg/ml), followed by the addition of 0.2-0.5 ml of NaReO₄ under a nitrogen atmosphere. The mixture was incubated at 80°C for 1 h. The labeling efficiency of the ^{188}Re -BMEDA complex was confirmed by paper chromatography with normal saline as the eluent. ^{188}Re -liposomes were prepared by adding 1 ml of liposomes to the ^{188}Re -BMEDA solution and incubated at 60°C for 30 min. The free ^{188}Re -BMEDA was removed using a PD-10 column (GE Healthcare) eluted with normal saline. The ^{188}Re -BMEDA loading efficiency was determined by taking the radioactivity in pegylated liposomes after separation divided by the total radioactivity before separation. ^{188}Re -DXR-liposome was prepared in the same way as ^{188}Re -liposome, 1 ml of 14.14 $\mu\text{mol/ml}$ of phospholipid Lipo-Dox (TTY Biopharm, Taipei, Taiwan) was mixed with ^{188}Re -BMEDA solution and incubated at 60°C for 30 min (10).

In vitro stability. The *in vitro* labeling stabilities of ^{188}Re -BMEDA with liposome and Lipo-Dox were studied comparably in normal saline and human plasma solution. After separation of ^{188}Re -(DXR)-liposome from free ^{188}Re -BMEDA complexes by PD-10 column, the *in vitro* labeling stability of ^{188}Re -(DXR)-liposome was evaluated by incubating ^{188}Re -(DXR)-liposome in normal saline (NS) (1:1 volume ratio) at room temperature and human plasma (1:19 volume ratio) at 37°C, respectively. At specific times after incubation, 150 µl of ^{188}Re -(DXR)-liposome solution were removed and the mixture separated on a column of Sepharose 4 Fast Flow (GE Healthcare) packed in a Poly-Prep chromatography column (Bio-Rad) using normal saline as eluent. The ^{188}Re -(DXR)-liposome was collected and counted using a Cobra II Auto-Gamma counter (Packard, USA). The labeling stability was calculated by dividing the ^{188}Re -(DXR)-liposome radioactivity by the total radioactivity (9, 11).

Biodistribution study. Nude mice were subcutaneously injected with HT-29 colorectal carcinoma cell line (2×10^6 cells) in the right hind flank. When tumor xenografts were fully established and had reached volumes of around 50 to 100 mm³, 1.85 MBq of ^{188}Re -BMEDA or ^{188}Re -(DXR)-liposome (phospholipid concentration 14.14 µmol/ml) were *i.v.* injected into each mice (n=5). At different times (1, 4, 16, 24 and 48 h) after *i.v.* injection, mice were sacrificed by CO₂ asphyxiation. Blood samples were collected through cardiac puncture. Organs of interest were removed, washed and weighed with radioactivity measured by a Cobra II Auto-Gamma counter. The results were expressed as the percentage of injected dose per gram of tissue (%ID/g).

Pharmacokinetic study. Pharmacokinetics of each blood sample were further calculated using WinNonlin software version 5.0.1 (Pharsight Corp., Mountain View, CA, USA). The parameters were calculated using noncompartmental analysis model 201 (*i.v.*-bolus input) with the log/linear trapezoidal rule. The pharmacokinetic parameters including area under the curve (AUC, h %ID/g), the maximum concentration (C_{max}, %ID/g), clearance (Cl, ml/h), and mean residence time (MRT, h) were calculated.

MicroSPECT/CT imaging. The SPECT images and CT images were acquired using a microSPECT/CT scanner (X-SPECT, Gamma Medica, Northridge, CA, USA). Mice were anesthetized with 1.5% isoflourine at 1, 4, 16, 24 and 48 h after *i.v.* injection of 18.5 MBq/200 µl of ^{188}Re -BMEDA and ^{188}Re -(DXR)-liposome. The source and detector are mounted on a circular gantry, allowing it to rotate 360° around the subject (mouse) positioned on a stationary bed. The radius of rotation was 1.0 cm with a field of view of 1.37 cm. The images were acquired using 64 projections at 90 s per projection. The energy window was set at 155 keV±10-15%. The SPECT imaging was followed by CT image acquisition (X-ray source: 50 kV, 0.4 mA; 256 projections) with the animal in exactly the same position.

WBAR imaging. After SPECT/CT imaging at 72 h, mice were sacrificed by CO₂ euthanasia and were immediately dipped into liquid nitrogen. The frozen carcasses were then embedded with 2.5% carboxymethyl cellulose (CMC). The frozen CMC block was attached to the sample stage in the cryochamber (−20°C). After 2 h, the frozen sample was then sectioned (40-µm-thick slices) using a cryomicrotome (CM 3600; Leica Instruments, Germany) at −20°C. These samples were placed in contact with an imaging plate (BAS-

MS 2040; Fuji Photo Film Co., Tokyo, Japan) for five days. After complete exposure, the imaging plate was analyzed with an FLA-5100 reader (Fuji Photo Film Co.) and Multi Gauge V3.0 software (Fuji Photo Film Co.).

Results

Preparation of ^{188}Re -BMEDA and ^{188}Re -(DXR)-liposome. The labeling efficiency of ^{188}Re -BMEDA complex was determined using ITLC-SG paper chromatography and was found to exceed 99%. The after-loading efficiency of ^{188}Re -liposome BMEDA in nanoliposome (^{188}Re -liposome) and Lipo-Dox (^{188}Re -DXR-liposome) were approximately 80±0.6% and 85.3±0.15% (n=3), respectively.

In vitro stability of ^{188}Re -(DXR)-liposome. *In vitro* stability of ^{188}Re -liposome and/or ^{188}Re -DXR-liposome at certain times after incubation in NS buffer at room temperature and 5% human serum-NS buffer at 37°C are shown in Figure 1a and b, respectively. The stability of ^{188}Re -liposome (n=3) and ^{188}Re -DXR-liposome (n=3) was 92.6±0.2 % and 77.5±2.3 % at 72 h, respectively in NS (Figure 1a), and 72.3±4.6 % and 60.2±9 % at 72 h, respectively, in 5% human serum (Figure 1b).

Biodistribution study. The %ID/g of ^{188}Re -BMEDA and ^{188}Re -(DXR)-liposome in blood, spleen, heart, liver, kidney, lung, tumor, feces and urine are presented in Figure 2, and the tumor to muscle (T/M) ratios are shown in Figure 3. The profiles of radiotherapeutics of ^{188}Re -liposome are similar to those of ^{188}Re -DXR-liposome, except that in spleen, but a significantly different profile was observed for ^{188}Re -BMEDA. The nanoliposomal drug formulation resulted in significantly higher uptake in blood, liver, spleen, tumor and lung than free did that of ^{188}Re -BMEDA. ^{188}Re -BMEDA exhibits fast blood clearance, and fast excretion from feces, urine and kidneys in 4 h after *i.v.* injection. In contrast, the uptake in tumor shows the tumor concentration for free ^{188}Re -BMEDA at 1 h after injection did not increase thereafter. ^{188}Re -liposome and ^{188}Re -DXR-liposome accumulation in the tumor was higher compared with free ^{188}Re -BMEDA, and resulted in the highest tumor to muscle uptake ratio at 14.4±2.7% and 17.1±4.1% at 24 h after injection, respectively.

Pharmacokinetic study. The area under the concentration–time curves in blood, liver, spleen, kidneys, heart and lungs after *i.v.* injection of ^{188}Re -liposome, ^{188}Re -DXR-liposome and free ^{188}Re -BMEDA are presented in Table I, and the pharmacokinetic parameters of drugs in blood are listed in Table II. ^{188}Re -liposome and ^{188}Re -DXR-liposome displayed a much greater systemic circulation time than did free ^{188}Re -BMEDA, which also showed rapid clearance kinetics and lower maximum concentration. The calculated AUCs of ^{188}Re -liposome and

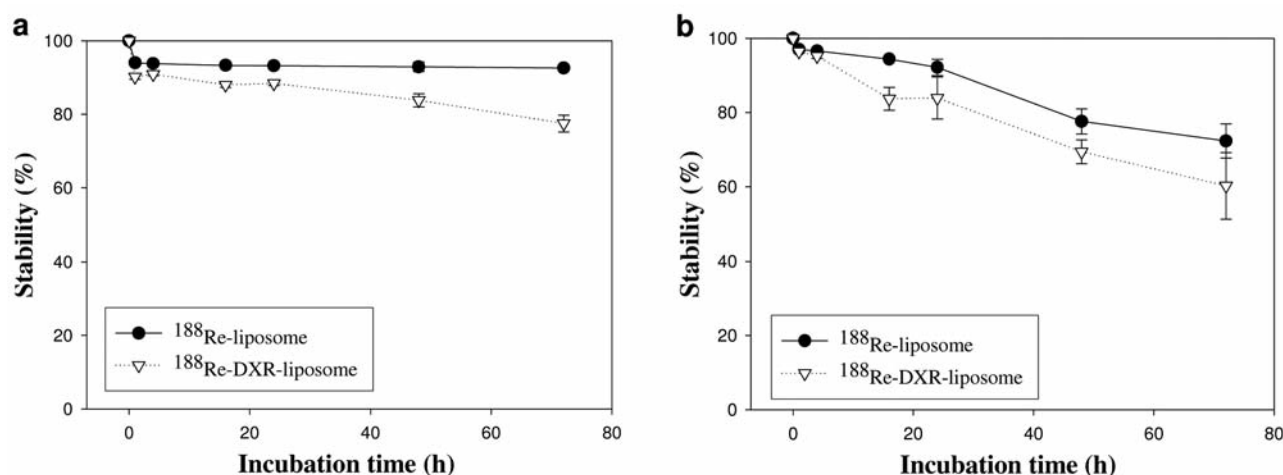


Figure 1. In vitro labeling stability of ^{188}Re -(DXR)-liposome at specific times after incubation in NS at room temperature (a) or human-NS plasma at 37°C (b) (mean \pm SEM, n=3).

Table I. AUC values in various tissues after i.v. injection of free ^{188}Re -BMEDA, and ^{188}Re -(DXR)-liposome into HT-29 tumor-bearing mice.

Formulation	Tissue AUC (h %ID/g)						
	Blood	Liver	Spleen	Kidney	Heart	Lung	Tumor
^{188}Re -BMEDA	73.63	221.4	54.46	128.1	41.45	41.45	15.71
^{188}Re -liposome	748.0	385.5	655.1	290.3	111.6	200.6	258.5
^{188}Re -DXR-liposome	577.9	377.3	3744	215.1	72.86	168.0	179.9

AUC values are calculated for 1-72 h.

^{188}Re -DXR-liposome were 10.2- and 7.8-fold higher than those of free ^{188}Re -BMEDA in blood, respectively. In addition, the nanoliposomal drug formulation also significantly increased AUC in liver, spleen, kidneys and lungs. However, a similar AUC was observed in heart for the three formulations. It is noteworthy that the mice treated with ^{188}Re -DXR-liposome had lower AUC values in blood, but showed significantly higher AUC values in spleen compared with those treated with ^{188}Re -liposome. The AUC value of tumor for ^{188}Re -liposome and ^{188}Re -DXR-liposome was 16.5- and 11.5-fold higher than that of free ^{188}Re -BMEDA, respectively.

MicroSPECT/CT and WBAR imaging. The SPECT/CT imaging of ^{188}Re -BMEDA indicates no significant uptake in tumor and other organs after i.v. injection, as shown in Figure 4. ^{188}Re -BMEDA was rapidly cleared and excreted from feces and urine in 4 h. However, the imaging of ^{188}Re -liposome and ^{188}Re -DXR-liposome showed accumulation in the liver, spleen and tumor after i.v. injection. Moreover, tumor uptake can be clearly seen at 16, 24 and 48 h. The autoradiography imaging

Table II. Pharmacokinetic parameters of ^{188}Re -BMEDA and ^{188}Re -(DXR)-liposome after i.v. injection in HT-29 tumor-bearing mice.

Parameter	^{188}Re -BMEDA	^{188}Re -liposome	^{188}Re -DXR-liposome
Cmax (%ID/g)	8.34	42.9	36.8
Cl (ml/h)	1.17	0.13	0.16
AUC (h %ID/g)	73.6	748	577
MRT (h)	10.5	14.1	13.7

Cmax: the maximum concentration; Cl: clearance; AUC: area under the curve; MRT: mean residence time.

was performed after the SPECT/CT image at 48 h (Figure 5). The WBAR obtained from coronal sections showed biodistribution of radiopharmaceutical similar to that obtained by SPECT/CT imaging. The tumor, spleen, liver and feces revealed the highest apparent accumulation of radioactivity at 48 h with ^{188}Re -(DXR)-liposome delivery. The WBAR can be employed to distinguish between the relative concentrations in each organ.

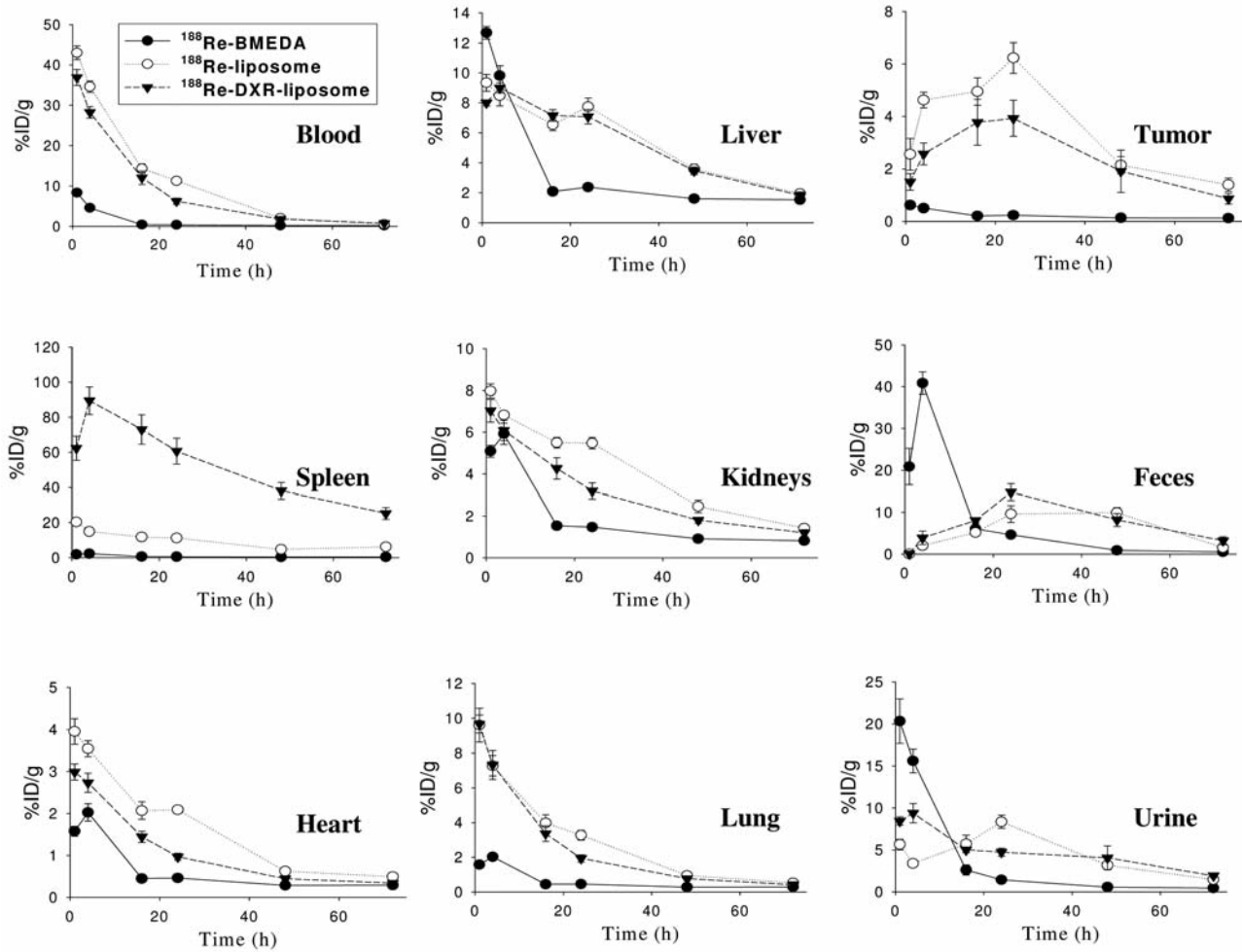


Figure 2. Biodistribution of free ^{188}Re -BMEDA, ^{188}Re -liposome, and ^{188}Re -DXR-liposome in various tissues after i.v. injection in HT-29 tumor-bearing mice. Mice were sacrificed at 1, 4, 16, 24, 48, and 72 h after drug administration. Results are given as the mean \pm SEM (n=5).

Discussion

To achieve nanoliposome labeling, radioisotopes can be attached to the surface of a liposome, embedded in double membrane of liposomes or encapsulated within the inner hydrophilic space of liposomes. An ideal liposome labeling method is the trapping of radioisotopes into the inner space of liposomes with high labeling efficiency and high specific activity using liposomes prepared before the radiolabeling procedure or radionuclide after-loading techniques (22, 25). The passively nanotargeted ^{188}Re -(DXR)-liposomes were prepared with similar after-loading techniques as reported previously (9, 11, 14, 19).

Liposome nanoparticles may represent the most effective nanocarriers for cancer chemotherapy. It has been shown that more than 98% of the drug is in liposome-encapsulated form after i.v. injection, indicating that the pharmacokinetics of liposomal doxorubicin are dictated by the liposome carrier

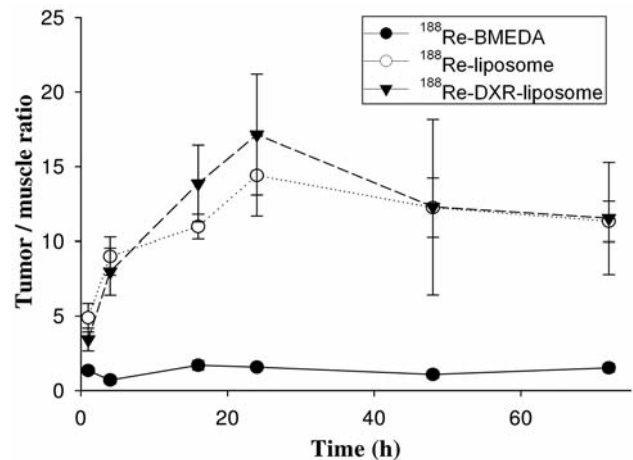


Figure 3. Uptake levels in tumor-to-muscle ratio of free ^{188}Re -BMEDA, ^{188}Re -liposome, and ^{188}Re -DXR-liposome after i.v. injection in HT-29 tumor-bearing mice from 0 to 72 h. Results are given as the mean \pm SEM (n=5).

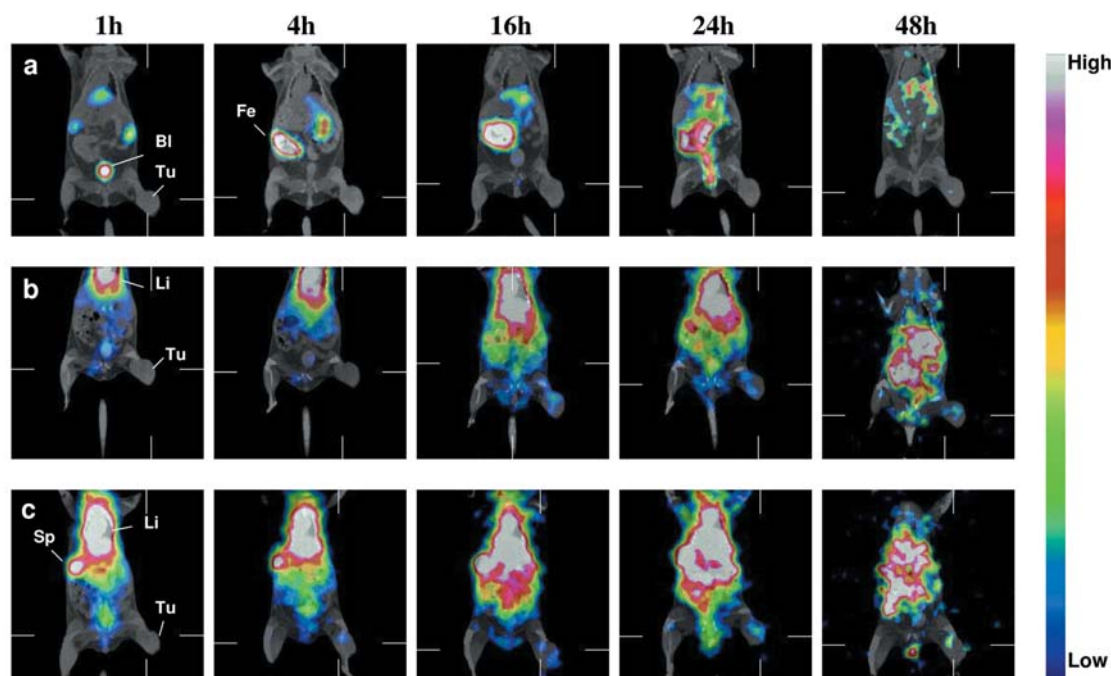


Figure 4. MicroSPECT/CT images of HT-29 tumor-bearing mice. Images of mice are shown at 1, 4, 16, 24 and 48 h after i.v. injection of ^{188}Re -BMEDA (a), ^{188}Re -liposome (b), and ^{188}Re -DXR-liposome (c). Li, Liver; Fe, feces; Sp, spleen; Bl, bladder; Tu, tumor.

and most of the drug is delivered to the tissue in liposome-associated form (26). These nanoparticles can be surface-grafted with PEG to prolong their systemic circulating half-life and enhance their tumor accumulation and therapeutic efficiency (27). Our results indicated that accumulation of ^{188}Re -liposomes and ^{188}Re -DXR-liposomes is 16.5- and 11.5-fold higher than that of ^{188}Re -BMEDA in tumor of HT-29 human solid tumor-bearing mice (Table I, Figure 2). The pharmacokinetics of ^{188}Re -(DXR)-liposome in the blood shows prolonged blood circulation, reduced clearance, an increased AUC, and an increased MRT of these passively nanotargeted radio/radiochemotherapeutics (Table II). In comparison with our previous studies (9, 14), the AUC ratios of nanotargeted radiotherapeutics of ^{188}Re -liposome to ^{188}Re -BMEDA was 10.2-fold (see Table II), which was larger than those seen in C26 solid tumor (4.6-fold) (9) and C26 ascites (6.8-fold) (14) mouse models. The imaging efficiency of these nanoliposomes in tumors was evaluated by accumulation and tumor to blood ratio obtained after administration of radio/radiochemotherapeutics to the mice (12), which was consistent with the tumor to muscle ratio obtained in this study (Figure 3). These results suggest that ^{188}Re -(DXR)-liposome may have better pharmacokinetics and higher bioavailability than ^{188}Re -BMEDA in human HT-29 xenografts, thus enhancing the level of tumor delivery via the EPR effect. Moreover, a high accumulation of passively nanotargeted therapeutics often results in enhanced therapeutic efficacy, minimal toxicity and side-effects (7).

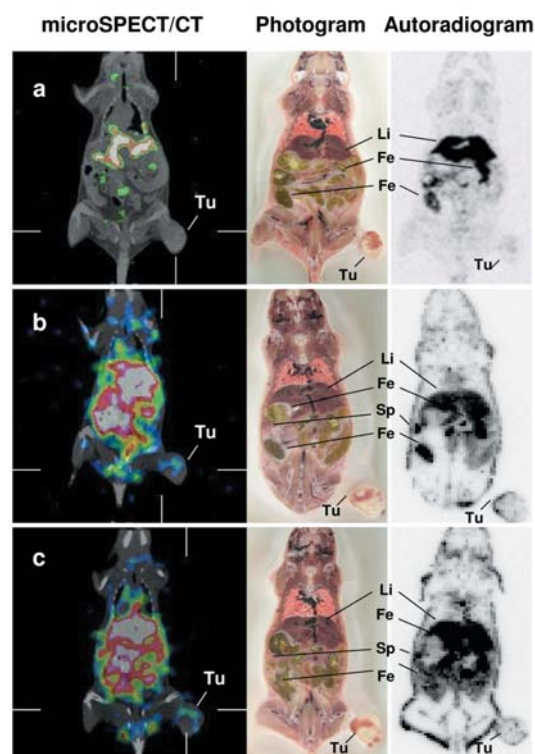


Figure 5. Coronal SPECT/CT image correlated with whole-body autoradiography in HT-29 tumor-bearing mice. Whole-body autoradiography imaging was performed at 48 h after i.v. injection of ^{188}Re -BMEDA (a), ^{188}Re -liposome (b), and ^{188}Re -DXR-liposome (c). Tu, Tumor; Li, liver; Fe, feces; Sp, spleen.

The applications of radionuclides encapsulated in nanoliposomes for imaging and internal radiotherapy have been discussed in previous reports (5, 28, 29). For diagnostic imaging, we have reported the bifunctional imaging and bimodality radiochemotherapeutic efficacy of ^{111}In -VNB-liposome in HT-29/luc-bearing mice (21, 30). Bao *et al.* used $^{99\text{m}}\text{Tc}$ -labeled Doxil to study non-invasive *in vivo* pharmacokinetics by gamma camera imaging (10, 31). The passively nanotargeted ^{188}Re -(DXR)-liposome tumor targeting was also confirmed by microSPECT/CT imaging (Figure 4) and validated by WBAR (Figure 5). The microSPECT/CT imaging provides faster dynamic non-invasive information for *in vivo* therapeutics tumor targeting and therapeutic response (Figure 4). ^{188}Re -(DXR)-liposome imaging revealed relatively long circulation in blood followed by retention in reticuloendothelial system of spleen and liver (Figure 5). The information of SPECT/CT imaging and WBAR correlated well with that obtained from biodistribution.

Our results showed that passively nanotargeted ^{188}Re -DXR-liposome has similar profile to that of ^{188}Re -liposome in mouse organs (Figure 2), and with significant uptake in the RES of spleen and liver. The enhanced uptake in liver and spleen is largely attributed to the macrophages residing in the tissues which are responsible for clearing liposome in the blood (7). Nanotargeted ^{188}Re -liposome and ^{188}Re -DXR-liposome at the 100-nm size range can passively accumulate in the tumor tissue site through the EPR effect. Following *i.v.* administration of the nanoliposomes, these predominantly accumulate in the interstitial fluid of extracellular and perivascular space of the tumor (32). Biodistribution and therapeutic index may be improved *via* an increase in polyethylene glycol (PEG) from 0.9% to 6% on passively nanotargeted ^{111}In -liposome in an HT-29/luc-xenografted mouse model (33). The nanoliposomal formulation of therapeutics diffused into the interstitial fluid of the tumor and RES may heavily affect the liposomal AUC in the blood stream. In comparison with our previous results on biodistribution, imaging and pharmacokinetics of ^{188}Re -liposome in the C26 tumor mouse model (9), similar findings were also obtained in the human HT-29 tumor-bearing animal models. In Taiwan, more information on the clinical application of ^{188}Re -liposome is needed. Translational research of passively nanotargeted radio/radiochemotherapeutics of ^{188}Re -(DXR)-liposome will be made in future therapeutic efficacy studies.

Conclusion

In vivo nuclear imaging, pharmacokinetics and biodistribution of passively nanotargeted radiotherapeutics of ^{188}Re -liposome and radiochemotherapeutics of ^{188}Re -DXR-liposome show that the high-energy β -emitters of ^{188}Re -labeled nanoliposomes have potential as a drug delivery system for improving the pharmacological and targeting properties of

radionuclides and drugs in the nude mouse model of human HT-29 solid colorectal adenocarcinoma. These results suggest that ^{188}Re -(DXR)-liposomes are potentially promising agents for use in treatment of malignant diseases.

Acknowledgements

The authors thank Dr. Tsai-Yueh Luo and Mr. Ching-Jun Liu for providing the rhenium-188, Mr. Wei-Chuan Hsu and Mr. Chung-Li Ho for their technical support in the animal biodistribution experiment, and Mr. Wei-Neng Liao for assistance in preparing the manuscript.

References

- 1 Jemal A, Siegel R, Ward E, Hao Y, Xu J, Murray T and Thun MJ: Cancer Statistics, 2008. *CA Cancer J Clin* 58: 71-96, 2008.
- 2 Liu YC, Sung FC, Hsieh LL, Tang R and Yeh CC: The risk prediction model and risk index for colorectal cancer. *Taiwan J Public Health* 27: 1-12, 2008.
- 3 Peer D, Karp JM, Hong S, Farokhzad OC, Margalit R and Langer R: Nanocarriers as an emerging platform for cancer therapy. *Nat Nanotechnol* 2: 751-760, 2007.
- 4 Messerer CL, Ramsay EC, Waterhouse D, Ng R, Simms EM, Harasym N, Tardi P, Mayer LD and Bally MB: Liposomal irinotecan: formulation development and therapeutic assessment in murine xenograft models of colorectal cancer. *Clin Cancer Res* 10: 6638-6649, 2004.
- 5 Hamoudeh M, Kamleh MA, Diab R and Fessi H: Radionuclides delivery systems for nuclear imaging and radiotherapy of cancer. *Adv Drug Deliv Rev* 60: 1329-1346, 2008.
- 6 Allen TM and Cullis PR: Drug delivery systems: entering the mainstream. *Science* 303: 1818-1822, 2004.
- 7 Li SD and Huang L: Pharmacokinetics and biodistribution of nanoparticles. *Mol Pharm* 5: 496-504, 2008.
- 8 Alberts DS, Muggia FM, Carmichael J, Winer EP, Jahanzeb M, Venook AP, Skubitz KM, Rivera E, Sparano JA, DiBella NJ, Stewart SJ, Kavanagh JJ and Gabizon AA: Efficacy and safety of liposomal anthracyclines in phase I/II clinical trials. *Semin Oncol* 31: 53-90, 2004.
- 9 Chang YJ, Chang CH, Chang TJ, Yu CY, Chen LC, Jan ML, Luo TY, Lee TW and Ting G: Biodistribution, pharmacokinetics and microSPECT/CT imaging of ^{188}Re -bMEDA-liposome in a C26 murine colon carcinoma solid tumor animal model. *Anticancer Res* 27: 2217-2225, 2007.
- 10 Bao A, Goins B, Klipper R, Negrete G and Phillips WT: Direct $^{99\text{m}}\text{Tc}$ labeling of pegylated liposomal doxorubicin (Doxil) for pharmacokinetic and non-invasive imaging studies. *J Pharmacol Exp Ther* 308: 419-425, 2004.
- 11 Bao A, Goins B, Klipper R, Negrete G and Phillips WT: ^{186}Re -liposome labeling using ^{186}Re -SNS/S complexes: *in vitro* stability, imaging, and biodistribution in rats. *J Nucl Med* 44: 1992-1999, 2003.
- 12 Ogihara-Umeda I, Sasaki T, Kojima S and Nishigori H: Optimal radiolabeled liposomes for tumor imaging. *J Nucl Med* 37: 326-332, 1996.
- 13 Iznaga-Escobar N: ^{188}Re -direct labeling of monoclonal antibodies for radioimmunotherapy of solid tumors: biodistribution, normal organ dosimetry, and toxicology. *Nucl Med Biol* 25: 441-447, 1998.

- 14 Chen LC, Chang CH, Yu CY, Chang YJ, Hsu WC, Ho CL, Yeh CH, Luo TY, Lee TW and Ting G: Biodistribution, pharmacokinetics and imaging of (188)Re-BMEDA-labeled pegylated liposomes after intraperitoneal injection in a C26 colon carcinoma ascites mouse model. *Nucl Med Biol* 34: 415-423, 2007.
- 15 Choy H and Kim DW: Chemotherapy and irradiation interaction. *Semin Oncol* 30: 3-10, 2003.
- 16 Huber PE, Bischof M, Jenne J, Heiland S, Peschke P, Saffrich R, Grone HJ, Debus J, Lipson KE and Abdollahi A: Trimodal cancer treatment: beneficial effects of combined antiangiogenesis, radiation, and chemotherapy. *Cancer Res* 65: 3643-3655, 2005.
- 17 Barbara Haley EF: Nanoparticles for drug delivery in cancer treatment. *Urologic Oncology: Seminars and Original Investigations* 26: 57-64, 2008.
- 18 Chang CH, Stabin MG, Chang YJ, Chen LC, Chen MH, Chang TJ, Lee TW and Ting G: Comparative dosimetric evaluation of nanotargeted ¹⁸⁸Re-(DXR)- liposome for internal radiotherapy. *Cancer Biotherapy and Radiopharmaceuticals* 23: 749-758, 2008.
- 19 Chen LC, Chang CH, Yu CY, Chang YJ, Wu YH, Lee WC, Yeh CH, Lee TW and Ting G: Pharmacokinetics, micro-SPECT/CT imaging and therapeutic efficacy of (188)Re-DXR-liposome in C26 colon carcinoma ascites mice model. *Nucl Med Biol* 35: 883-893, 2008.
- 20 Carlson SK, Classic KL, Hadac EM, Bender CE, Kemp BJ, Lowe VJ, Hoskin TL and Russell SJ: *In vivo* quantitation of intratumoral radioisotope uptake using micro-single photon-emission computed tomography/computed tomography. *Mol Imaging Biol* 8: 324-332, 2006.
- 21 Lee WC, Hwang JJ, Tseng YL, Wang HE, Chang YF, Lu YC, Ting G, Whang-Peng J and Wang SJ: Therapeutic efficacy evaluation of ¹¹¹In-VNB-liposome on human colorectal adenocarcinoma HT-29/luc mouse xenografts. *Nucl Instrum Methods Phys Res Sect A* 569: 497-504, 2006.
- 22 Tseng YL, Hong RL, Tao MH and Chang FH: Sterically stabilized anti-idiotypic immunoliposomes improve the therapeutic efficacy of doxorubicin in a murine B-cell lymphoma model. *Int J Cancer* 80: 723-730, 1999.
- 23 Bartlett GR: Phosphorus assay in column chromatography. *J Biol Chem* 234: 466-468, 1959.
- 24 Hsieh BT, Callahan AP, Beets AL, Ting G and Knapp Jr FF: Ascorbic acid/saline eluant increases ¹⁸⁸Re yields after wet storage of ¹⁸⁸W/¹⁸⁸Re generators. *Appl Radiat Isot* 47: 23-26, 1996.
- 25 Tilcock C: Delivery of contrast agents for magnetic resonance imaging, computed tomography, nuclear medicine and ultrasound. *Adv Drug Deliv Rev* 37: 33-51, 1999.
- 26 Gabizon A, Catane R, Uziely B, Kaufman B, Safran T, Cohen R, Martin F, Huang A and Barenholz Y: Prolonged circulation time and enhanced accumulation in malignant exudates of doxorubicin encapsulated in polyethylene-glycol coated liposomes. *Cancer Res* 54: 987-992, 1994.
- 27 Alexis F, Rhee JW, Richie JP, Radovic-Moreno AF, Langer R and Farokhzad OC: New frontiers in nanotechnology for cancer treatment. *Urol Oncol* 26: 74-85, 2008.
- 28 Ting G, Chang CH and Wang HE: Cancer nanotargeted radiopharmaceuticals for tumor imaging and therapy. *Anticancer Res* 29: 4107-4118, 2009.
- 29 Phillips WT, Goins B and Bao A: Radioactive liposomes. *Wiley Interdiscipl Rev Nanomed Nanobiotechnol* 1: 69-83, 2009.
- 30 Chow TH, Lin YY, Hwang JJ, Wang HE, Tseng YL, Pang VF, Wang SJ, Whang-Peng J and Ting G: Diagnostic and therapeutic evaluation of (111)In-vinorelbine-liposomes in a human colorectal carcinoma HT-29/luc-bearing animal model. *Nucl Med Biol* 35: 623-634, 2008.
- 31 Goins BA: Radiolabeled lipid nanoparticles for diagnostic imaging. *Expert Opin Med Diagn* 2: 853-873, 2008.
- 32 Park JW, Kirpotin DB, Hong K, Shalaby R, Shao Y, Nielsen UB, Marks JD, Papahadjopoulos D and Benz CC: Tumor targeting using anti-her2 immunoliposomes. *J Control Release* 74: 95-113, 2001.
- 33 Chow TH, Lin YY, Hwang JJ, Wang HE, Tseng YL, Wang SJ, Liu RS, Lin WJ, Yang CS and Ting G: Improvement of biodistribution and therapeutic index *via* increase of polyethylene glycol on drug-carrying liposomes in an HT-29/luc xenografted mouse model. *Anticancer Res* 29: 2111-2120, 2009.

Received July 25, 2009

Revised November 16, 2009

Accepted November 25, 2009